R. & M. No. 3315

MINISTRY OF AVIATION

AERONAUTICAL RESEARCH COUNCIL
REPORTS AND MEMORANDA

Measurements of Pitching-Moment Derivatives for Blunt-Nosed Aerofoils Oscillating in Two-Dimensional Supersonic Flow

By P. G. PUGH, B.Sc. and L. WOODGATE,
OF THE AERODYNAMICS DIVISION, N.P.L.

LONDON: HER MAJESTY'S STATIONERY OFFICE
1963
EIGHT SHILLINGS NET

Measurements of Pitching-Moment Derivatives for Blunt-Nosed Aerofoils Oscillating in Two-Dimensional Supersonic Flow

By P. G. PUGH, B.Sc. and L. WOODGATE,
OF THE AERODYNAMICS DIVISION, N.P.L.

*Reports and Memoranda No. 3315**
July, 1961

Summary.

Direct pitching-moment derivatives have been measured using the method of Scruton, Woodgate *et al*[2] for two single-wedge blunt-nosed aerofoils. These measurements were made at Mach numbers of 1·75 and 2·47 and frequency parameters less than 0·02. In general, nose blunting was found to have little effect on the derivatives although changes were observed for the thinner wedge at a Mach number of 1·75.

1. *Introduction.*

This report describes measurements made to investigate the effects of nose blunting on the direct pitching derivatives for single-wedge aerofoils oscillating in supersonic flow. The aerofoils tested were generated from two single-wedge sharp-nosed models, of thickness/chord ratios of 16% and 24%, whose leading edges were rounded to have various radii. These aerofoils had an original chord length of 2·5 in., the largest leading-edge radii applied being 0·050 in. and 0·070 in. for the 16% and 24% thick wedges respectively. Tests were made at a frequency of approximately 20 c/s at Mach numbers of 1·75 and 2·47 with 30 in. mercury stagnation pressure; thus giving frequency parameters of approximately 0·15 and 0·12 while the Reynolds numbers were approximately $8{\cdot}8 \times 10^5$ and $6{\cdot}6 \times 10^5$ at the Mach numbers of 1·75 and 2·47 respectively. Measurements were made using an essentially similar technique to that described by Scruton and Woodgate[2] the aerodynamic derivatives being estimated from records of decaying pitching oscillations of the aerofoil.

In general little difference was noted between derivatives for the sharp-nosed and blunt-nosed configurations but some influence of leading-edge bluntness was noted for the thinner wedge at the lower Mach number. It was also noted that theoretical values calculated using Lighthill's piston theory[6] were in good agreement with the measured values for the sharp-nosed wedges.

In computing m_θ, $m_{\dot\theta}$ actual values of c' appropriate to each model configuration have been used and it is this length that was used in obtaining a non-dimensional form of the distance of the pitching axis behind the aerofoil leading edge.

* Replaces A.R.C. 23,012. Published with the permission of the Director, National Physical Laboratory.

2. *Basic Formulae.*

The aerodynamic moment acting on the aerofoil may be expressed as:

$$\mathscr{M} = M_\theta\theta + M_{\dot\theta}\dot\theta$$

and for simple harmonic motions of frequency $f = \omega/2\pi$ $\mathscr{M}$ may be expressed in terms of its in-phase and quadrature components as

$$\mathscr{M} = \rho V^2 c'^2 s(m_\theta + j\nu m_{\dot\theta})\theta$$

where $j = \sqrt{-1}$ and $\nu = \omega c'/V$. The equation of motion for the aerofoil performing free oscillations in a pitching motion against a spring constraint is then

$$I\ddot\theta + (K + M_{\dot\theta})\dot\theta + (\sigma - M_\theta)\theta = 0.$$

Using the solution

$$\theta = \theta_0 e^{\mu t}\sin\omega t$$

and assuming, as is generally true for such experiments, that $\mu^2 - \mu_0^2 \ll \omega^2 - \omega_0^2$ and $\mu_0^2 \ll \omega_0^2$ then:

$$M_\theta = \frac{\sigma}{f_0}(f - f_0)(f + f_0)$$

$$M_{\dot\theta} = 2I(f\delta - f_0\delta_0).$$

3. *Description of Apparatus.*

The Wind Tunnel.

These tests were conducted in the N.P.L. 14 × 11 in. High Speed Tunnel[1]. This tunnel is of the continuous-flow type being driven by an axial-flow compressor capable of producing a maximum Mach number of 2·5 at the maximum stagnation pressure of 1 atmosphere. In order to keep the tunnel air as dry as possible, and also to regulate the stagnation pressure, air was continuously extracted from the tunnel by vacuum pumps, this air being replaced by dry air. The rate of injection of this dry air was adjusted so as to maintain a constant stagnation pressure. By this means the first point of the tunnel was held below a maximum of − 15°F this value having been found in previous tests[2] to be amply sufficient for the avoidance of any humidity effects.

Models Tested.

Two single-wedge aerofoil models were constructed by machining from solid 'Leadloy' steel plate. These were of 2·5 in. chord, had sharp leading edges, and were of 16% and 24% thickness/chord ratios. The models completely spanned the tunnel and were provided with rectangular-section flanges for bolting the aerofoil to the support gear. Other, blunt-nosed, configurations were produced by machining circular-arc noses, of various radii, onto these wedges maintaining a continuous variation of slope over each surface. The configurations used are shown in Fig. 1.

Support Gear.

The model support gear was mechanically identical to that used for the earlier investigation by Scruton, Woodgate *et al*[2] and is shown in Fig. 2. The aerofoil was supported, by two similar mountings, on either side of the tunnel. These mountings consisted, in essentials, of a cylinder suspended on two sets of cross-spring bearings which constrained the cylinder to rotate about its longitudinal axis without transverse motion. Rotation of this cylinder was opposed by a torque bar 'B' providing angular stiffness sufficient to give the suspended system a natural frequency of approximately 20 c/s. Aerofoils were mounted in this apparatus by bolting the rectangular-section flanges, mentioned earlier, to the end of the cylinder 'A'. These flanges also carried two circular discs 'D' which, rotating with the aerofoil, replaced part of the tunnel wall. The gap between these

discs and the tunnel wall was small and air leakage into the tunnel was prevented by enclosing the complete support gear in an airtight box. Accordingly it was considered that negligible interference was caused to the flow inside the tunnel. The aerofoil was thus free to rotate about a fixed axis passing through its chord line. Such a motion could be excited using a spring-mounted plunger to displace the model and alternative pitching axes could be obtained by movement of the aerofoil along the tunnel to other sets of bolt holes for its attachment to the cylinder 'A'.

Reflection of light beams from small mirrors mounted on each cylinder 'A' gave, by means of the movement of a light spot over a large scale, a visual indication of the displacement. This indication was useful in confirming that the aerofoil torsional stiffness was sufficient to avoid undesirable effects due to the asymmetric excitation; and also provided, *via* a photocell, pulse signals used in frequency measurement.

Measurement and Analysis of Results.

The results were obtained and analysed by the methods used by Woodgate, Maybrey and Scruton[3] in their recent measurements of three-dimensional wing derivatives. The angular displacement of the model from its zero-incidence equilibrium position was indicated by a shift of the light spot, mentioned earlier, and measured using a simple condenser gauge. A d.c. voltage proportional to this angular displacement was produced by coupling the gauge to Southern Instruments frequency-modulation equipment, and displayed on one beam of a double-beam oscilloscope. The other C.R.O. beam was fed with time pulses at 0·01 sec intervals generated by a Dekatron frequency divider from the standard N.P.L. 1 kc/s frequency supply. A film record was made of each test using a continuously moving film camera to photograph the C.R.O. screen. Calibration traces were inserted on the record after each experiment, being obtained by the static deflection of the model to various displacements as indicated by the movement of the light spot.

These records are sufficient for the estimation of stiffness and damping forces acting on the model and as such were used by Scruton and Woodgate[2]. However, in subsequent tests[3] it has been found convenient to avoid the laborious direct counting of cycles necessary for extraction of frequencies from each record. Thus while the time-marker pulses were retained the periodic time of the oscillations was measured during each test using a Dekatron counter. This instrument received both the 1 kc/s N.P.L. supply and pulses generated by movement of the light spot across a small photocell at the centre of one scale. By counting the number of 1 kc/s pulses occurring during the arrival of 100 photocell pulses this counter directly measured the periodic time of model oscillation. Adjustment of the photocell position prior to each test ensured that each pulse was delivered as the aerofoil passed through its equilibrium position. The use of this second pulsed output thus avoided difficulties in accurate automatic frequency measurement due to the decaying nature of the oscillation. A schematic diagram of this equipment is given in Fig. 3.

The logarithmic decrement of the oscillation was obtained by analysis of film records in the manner previously utilised[2], and the elastic stiffness was measured by a dead-weight method.

4. *Method of Test.*

Records of the decaying oscillations of the aerofoil were obtained in wind using the equipment described in the previous section. This test was then repeated without airflow past the aerofoil and the tunnel evacuated to approximately 10 in. mercury pressure. This was the minimum pressure attainable; however, previous experience[2] had shown that the apparatus damping was insensitive to ambient pressure.

Since the elastic stiffness had been determined in a static experiment, the stiffness and damping experienced by the aerofoil during each test could be estimated and the aerodynamic contribution found by difference.

5. *Discussion of Results.*

The aerodynamic stiffness and damping derivatives measured are plotted against relative axis position (h) in Figs. 4 to 11 and Tables 1 and 2. It will be observed that theoretical and experimental results are in reasonable quantitative agreement for the sharp-nosed aerofoils under all test conditions, and that virtually no systematic changes are produced in the stiffness derivatives by increasing nose bluntness. A small decrease of the minimum value of the aerodynamic damping derivative is observable with nose blunting but again no large changes occur except for the thinner wedge at the lower Mach number, where its occurrence is puzzling.

For all values of nose radius adopted during these tests the ratio of nose radius to model chord is small, thus the blunt nose may be expected to influence the aerodynamic loads on the aerofoil by virtue of its disturbance of downstream flow rather than directly due to the pressure distribution around it.

On the basis of work due to Meyer[5] it has been suggested by Lighthill[4] that the considerable entropy changes experienced by air passing through the detached bow shock would not substantially affect surface pressures over a blunt-nosed body. Thus since the sonic point is, for all reasonable values of incidence, situated on the circular-section nose, and since this nose shape is invariant under rotation Lighthill suggested[4] that the influence of a small blunt leading edge on the static lift would be negligible. This clearly implies that for the quasi-static flow to be expected at the low frequency parameter of these tests, a blunt leading edge is unlikely to have any significant influence on the stiffness derivative It may also be argued that no departure from the parabolic shape of the damping derivative against axis-position curve, is to be expected providing the nose is small and lack of isentropy unimportant.

These contentions are well borne out by the experimental results except, as noted earlier, for the thinner wedge at a Mach number of 1·75 (the lower Mach number). It is surprising that nose blunting should be important only under those circumstances when entropy changes would be expected to be smallest and for axis positions forward of mid-chord where changes in the pressure distribution near the nose would be expected to have least effect. In an attempt to locate the source of this anomaly, shadow and schlieren photographs were taken for each model configuration with the model held fixed at 0° and 5° incidence. No features differing from those seen for other configurations and test conditions were observed, however, in the flow around the thinner wedge at a Mach number of 1·75. It would appear, therefore, most likely that the problem is not quasi-static. At the low frequency parameter of these tests a small variation in the angle of lag between displacement and moment such as would not significantly alter the stiffness derivative would change the damping derivative considerably. Further investigations are necessary in order to determine the cause of the effect.

Pitching-moment derivatives were computed using the piston theory of Lighthill[6] for the blunt-nosed wedges as well as for the simple single wedges. As was to be expected little difference was noted between sharp- and blunt-nosed derivatives, the blunting increasing slightly the damping derivative for axis positions aft of mid-chord.

6. *Conclusion.*

The results obtained indicate that, at the test Mach numbers (1·75 and 2·47), substantial amounts of nose blunting do not in general markedly affect the direct pitching derivatives ($-m_\theta$, $-m_{\dot{\theta}}$) for a single-wedge aerofoil. However, some reduction in ($-m_{\dot{\theta}}$) was noted for the thinner wedge at $M = 1{\cdot}75$. It was concluded that the flow pattern was probably non-quasi-static in this case.

The agreement between piston theory and experiment, noted in earlier tests[2], for sharp-nosed single-wedge aerofoils was confirmed.

7. *Acknowledgements.*

The authors are greatly indebted to Mr. W. E. Acum for his invaluable assistance in the application of piston theory to the model configurations tested; and also to Miss W. Scott who performed most of the computational work involved.

NOTATION

M	Mach number
V	Wind speed
ρ	Air density
c	Original (sharp-edged) aerofoil chord
c'	Aerofoil chord
s	Aerofoil span
I	Moment of inertia of oscillating system
K	Apparatus damping
σ	Elastic angular stiffness opposing displacement of oscillating system
$-M_\theta$	Aerodynamic stiffness derivative
$-M_{\dot\theta}$	Aerodynamic damping derivative
$-m_\theta = \frac{-M_\theta}{\rho V^2 c'^2 s}$	; non-dimensional form of $-M_\theta$
$-m_{\dot\theta} = \frac{-M_{\dot\theta}}{\rho V c'^3 s}$	; non-dimensional form of $-M_{\dot\theta}$
f	Frequency of oscillation
ω	Circular frequency $= 2\pi f$
δ	Logarithmic decrement of oscillation
θ	Angular displacement in pitching motion
hc'	Distance of pitching axis behind the leading edge of the aerofoil
	Suffix $_0$ applied to the quantities for tests *in vacuo*.

REFERENCES

No.	*Author*	*Title, etc.*
1	G. A. Hawkins and W. F. Cope	The flow of gases at sonic and supersonic speeds. *Proc. Inst. Mech. Eng.* (*App. Mech.*). Vol. 155. 1946.
2	C. Scruton, L. Woodgate, K. C. Lapworth and J. F. M. Maybrey	Measurement of pitching-moment derivatives for aerofoils oscillating in two-dimensional supersonic flow. A.R.C. R. & M. 3234. January, 1959.
3	L. Woodgate, J. F. M. Maybrey and C. Scruton	Measurement of pitching-moment derivatives for rigid tapered wings of hexagonal planform oscillating in supersonic flow. A.R.C. R. & M. 3294. March, 1961.
4	M. J. Lighthill	*General theory of high-speed aerodynamics.* Section E5. Oxford University Press. 1955.
5	R. E. Meyer	The method of characteristics for problems of compressible flow involving two independent variables. Part I. The general theory. *Quart. J. Mech. App. Math.* Vol. 1. pp. 196 to 219. 1948.
6	M. J. Lighthill	Oscillating aerofoils at high Mach number. *J. Ae. Sci.* Vol. 20. June, 1953.
7	M. D. Van Dyke	Supersonic flow past oscillating airfoils including nonlinear thickness effects. N.A.C.A. Report 1183. 1954.

APPENDIX

After the completion of this report Miss D. Lehrian drew the attention of the authors to the extremely good agreement between their measured derivatives and those calculated by her using Van Dyke's theory[7]. A comparison of these results with measured values and those calculated using piston theory is given in Figs. A1 to A4.

It can be seen from these figures that use of Van Dyke's theory gives values more in accord with experimental observation than the use of piston theory. It is also worth note that the errors inherent in the application of piston theory increase with increasing aerofoil thickness and decreasing Mach number. The results therefore give some indication of a Mach number thickness boundary for the employment of piston theory. The direct use of such a limited number of results cannot however be hoped to give any precise form or meaning to such a boundary. Current work by the authors, however, has employed a correlation of these and earlier results, based on mean flow conditions behind the bow shock wave; and it is hoped to discuss in a later paper the use of this correlation to obtain more precise bounds to the applicability of piston theory.

The authors are most grateful to Miss D. Lehrian for her help and advice in this work.

TABLE 1

Measured and theoretical values of the derivatives $-m_\theta$, $-m_{\dot\theta}$ for a single-wedge aerofoil of original thickness/chord ratio 24% at zero mean incidence

r (in.)	M	h	Experimental		Piston Theory	
			$-m_\theta$	$-m_{\dot\theta}$	$-m_\theta$	$-m_{\dot\theta}$
0	2·47	0·00	0·61	0·17	0·548	0·363
		0·25	0·31	0·08	0·276	0·157
		0·50	0·00	0·09	0·004	0·087
		0·75	−0·29	0·20	−0·268	+0·153
		1·00	−0·58	0·57	−0·540	0·355
0	1·75	−0·25	1·29	0·36		
		0·00	0·87	0·05	0·648	0·466
		0·25	0·44	−0·04	0·324	0·204
		0·50	0·01	0·04	0·000	0·117
		0·75	−0·43	0·33	−0·324	0·208
		1·00	−0·89	0·79	−0·648	0·466
0·025	2·47	−0·08	0·68	0·25	0·641	0·459
		0·19	0·36	0·11	0·346	0·194
		0·46	0·05	0·05	0·051	0·087
		0·73	−0·26	0·20	−0·242	0·138
		1·00	−0·56	0·55	−0·536	0·348
0·025	1·75	−0·08	0·99	0·10	0·817	0·589
		0·19	0·54	−0·05	0·431	0·254
		0·46	0·08	−0·01	0·045	0·127
		0·73	−0·39	0·39	−0·341	0·206
		1·00	−0·84	0·77	−0·727	0·493
0·050	2·47	−0·17	0·78	0·31	0·751	0·587
		0·12	0·44	0·12	0·416	0·239
		0·41	0·10	0·05	0·083	0·074
		0·71	−0·22	0·17	−0·250	0·094
		1·00	−0·55	0·56	−0·584	0·297
0·050	1·75	−0·17	1·17	0·31	0·945	0·755
		+0·12	0·67	−0·04	0·530	0·360
		+0·41	0·17	−0·06	0·104	0·133
		+0·71	−0·33	0·27	−0·321	0·238
		+1·00	−0·82	0·76	−0·746	0·510
0·070	2·47	−0·26	0·87	0·45	0·856	0·725
		0·05	0·53	0·11	0·490	0·301
		0·37	0·16	0·04	0·123	0·107
		0·68	−0·19	0·14	−0·243	0·145
		1·00	−0·56	0·52	−0·610	0·414
0·070	1·75	−0·26	1·32	0·52	1·087	0·930
		0·05	0·79	0·10	0·622	0·391
		0·37	0·25	−0·09	0·158	0·145
		0·68	−0·28	0·17	−0·307	0·192
		1·00	−0·80	0·72	−0·772	0·532

(86603) A*

TABLE 2

Measured and theoretical values of the derivatives $-m_\theta$, $-m_{\dot\theta}$ for a single-wedge aerofoil of original thickness/chord ratio 16% at zero mean incidence

r (in.)	M	h	Experimental		Piston Theory	
			$-m_\theta$	$-m_{\dot\theta}$	$-m_\theta$	$-m_{\dot\theta}$
0	2·47	−0·25	0·83	0·54		
		0·00	0·55	0·19	0·497	0·331
		0·25	0·27	0·08	0·248	0·145
		0·50	0·00	0·06	0·000	0·082
		0·75	−0·28	0·20	−0·248	0·145
		1·00	−0·55	0·47	−0·497	0·331
		+1·25	−0·83	0·84		
0	1·75	−0·25	1·21	0·77		
		0·00	0·81	0·31	0·652	0·435
		+0·25	0·40	0·03	0·325	0·185
		0·50	0·00	0·03	0·000	0·109
		0·75	−0·41	0·32	−0·325	0·190
		1·00	−0·81	0·76	−0·652	0·435
		1·25	−1·20	1·28		
0·025	2·47	−0·131	0·66	0·34	0·636	0·506
		+0·152	0·35	0·08	0·345	0·205
		+0·435	0·06	0·04	0·055	0·097
		0·717	−0·25	0·18	−0·234	0·150
		1·000	−0·52	0·46	−0·524	0·376
0·025	1·75	−0·131	0·97	0·32	0·824	0·546
		−0·152	0·54	0·02	0·450	0·232
		+0·435	0·10	0·01	0·075	0·102
		0·717	−0·33	0·26	−0·300	0·158
		1·000	−0·76	0·69	−0·674	0·398
0·050	2·47	−0·300	0·83	0·36	0·821	0·731
		+0·025	0·48	0·17	0·477	0·309
		0·350	0·15	0·03	0·133	0·111
		0·675	−0·17	0·14	−0·211	0·136
		1·000	−0·51	0·53	−0·555	0·384
0·050	1·75	−0·300	1·23	0·40	1·063	0·948
		+0·025	0·73	0·09	0·623	0·402
		0·350	0·24	0·03	0·179	0·142
		0·675	−0·26	0·18	−0·262	0·169
		1·000	−0·85	0·65	−0·705	0·483

Cross–section of model

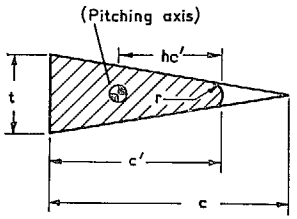

Original chord = 2·5″ = c

1) Original (sharp–nosed) thickness / chord ratio = 16%

	r	c′	t / c′
a)	0	2·5″	16%
b)	0·025″	2·211″	18·1%
c)	0·050″	1·923″	20·8%

2) Original (sharp–nosed) thickness/chord ratio = 24%

	r	c′	t/c′
a)	0	2·5″	24%
b)	0·025″	2·315″	25·9%
c)	0·050″	2·130″	28·2%
d)	0·070″	1·982″	31·1%

FIG. 1. Model configurations tested.

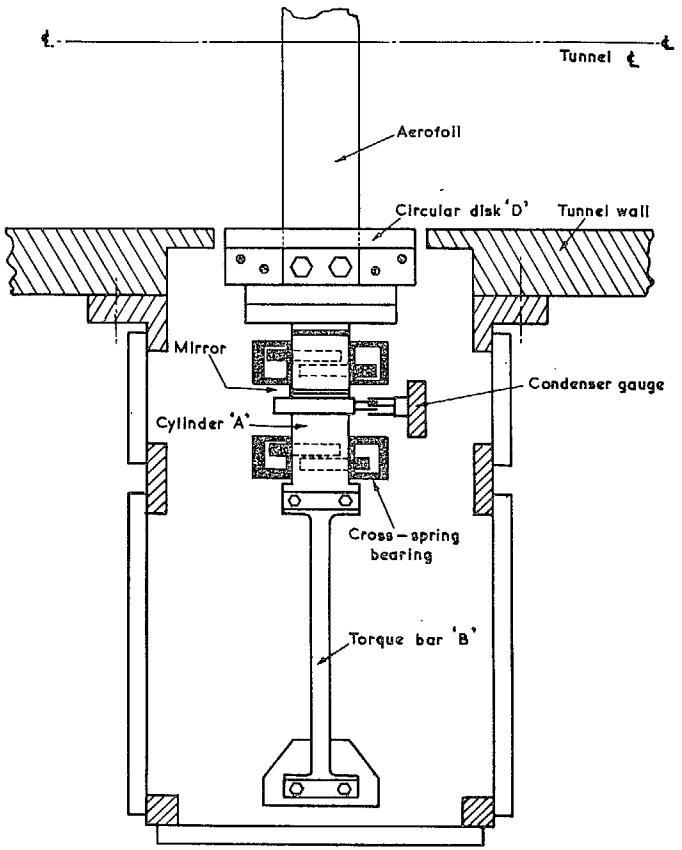

FIG. 2. Schematic plan view of model and spring bearing.

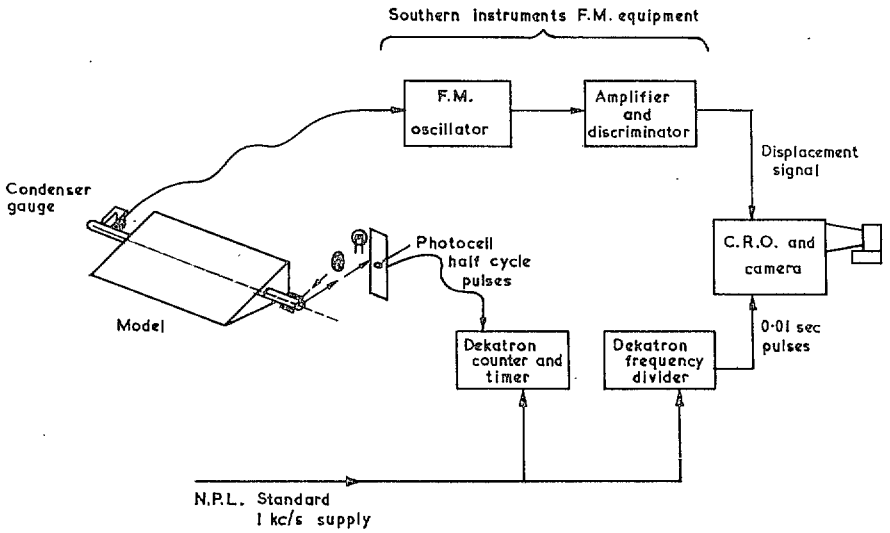

FIG. 3. Schematic diagram of measuring and recording apparatus.

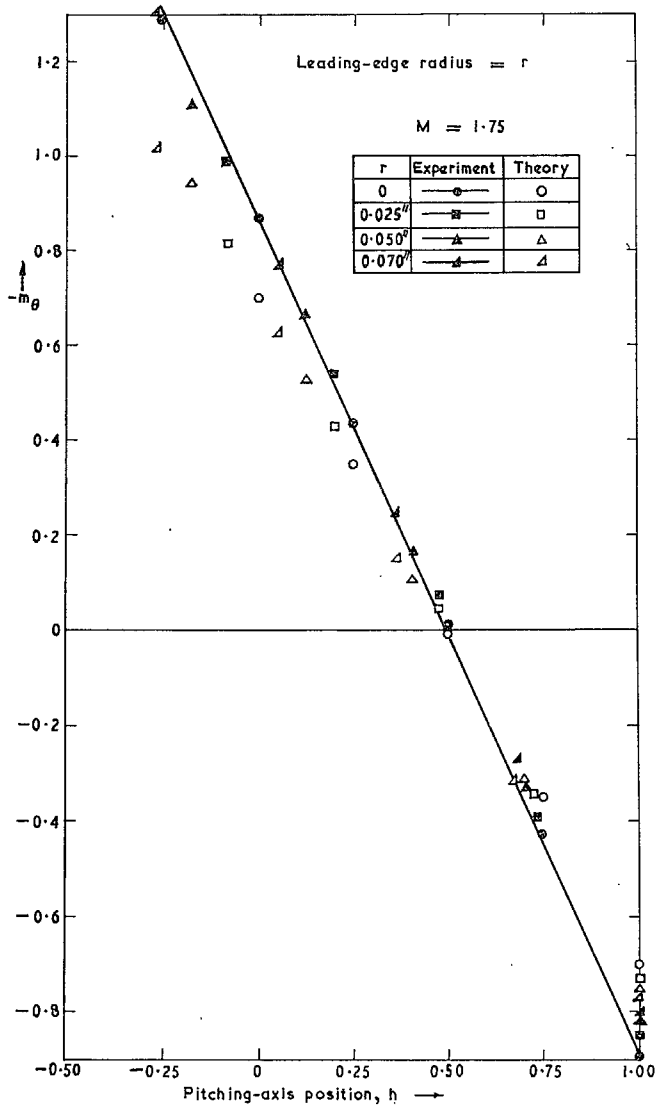

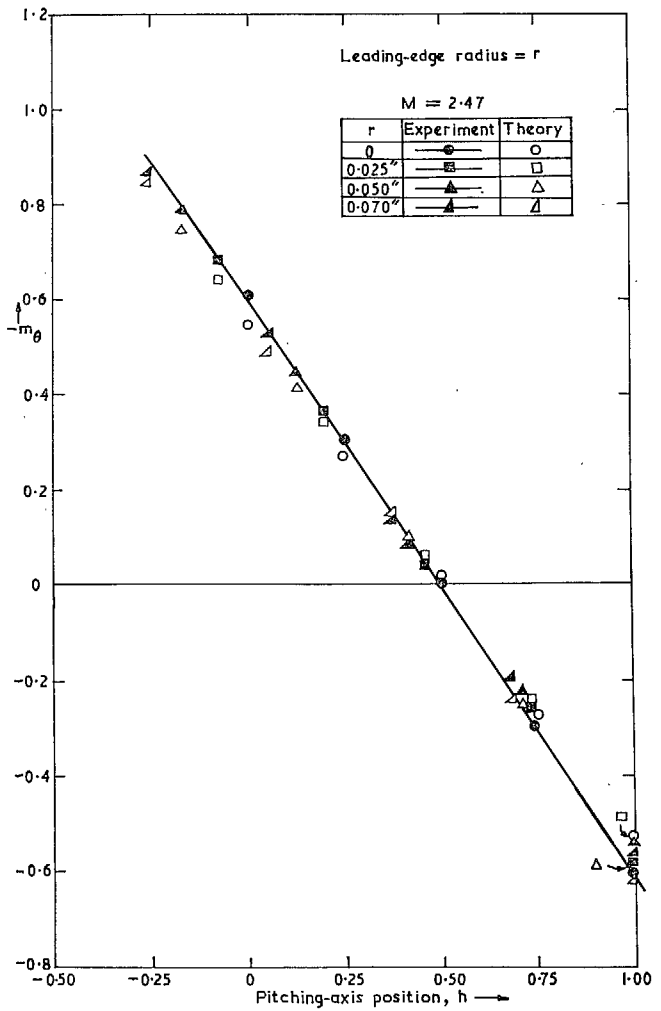

FIGS. 4 and 5. Direct pitching aerodynamic stiffness ($-m_\theta$) for blunt-nosed 24% thick single-wedge aerofoil.

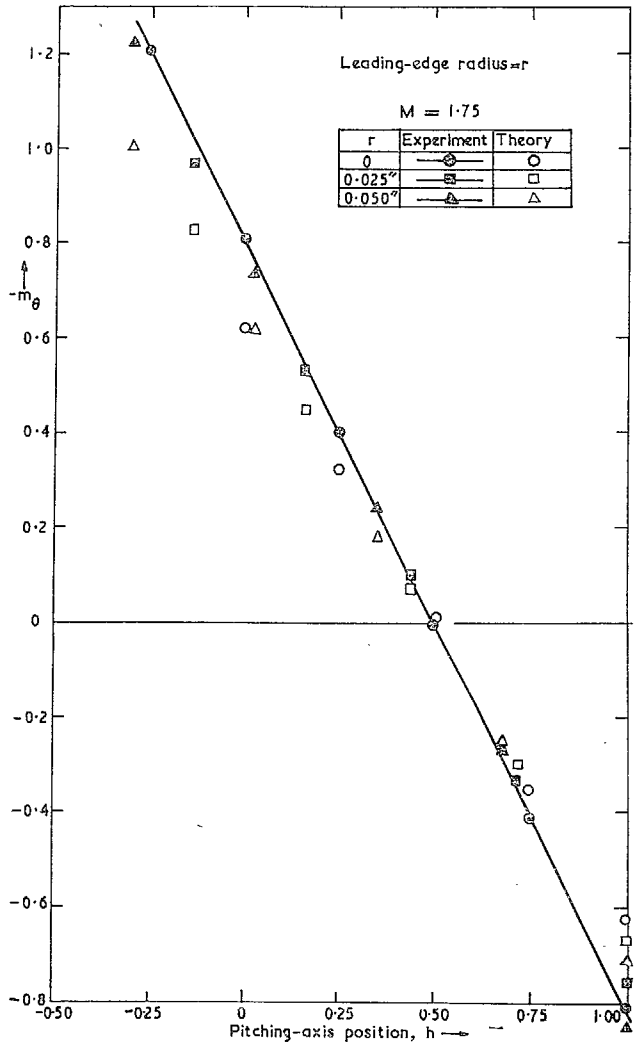

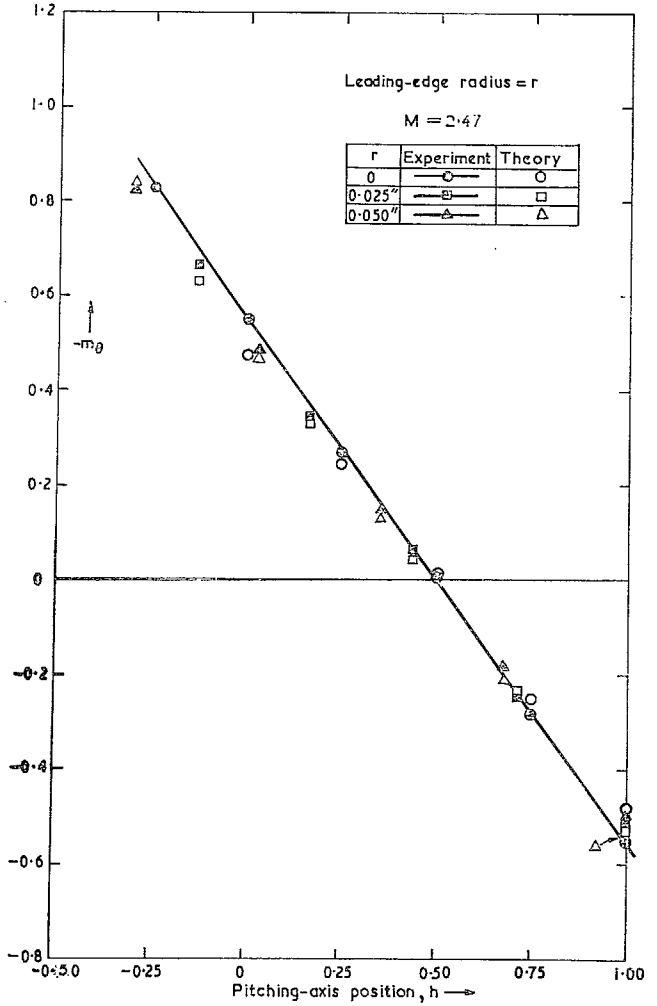

FIGS. 6 and 7. Direct pitching aerodynamic stiffness ($-m_\theta$) for blunt-nosed 16% thick single-wedge aerofoil.

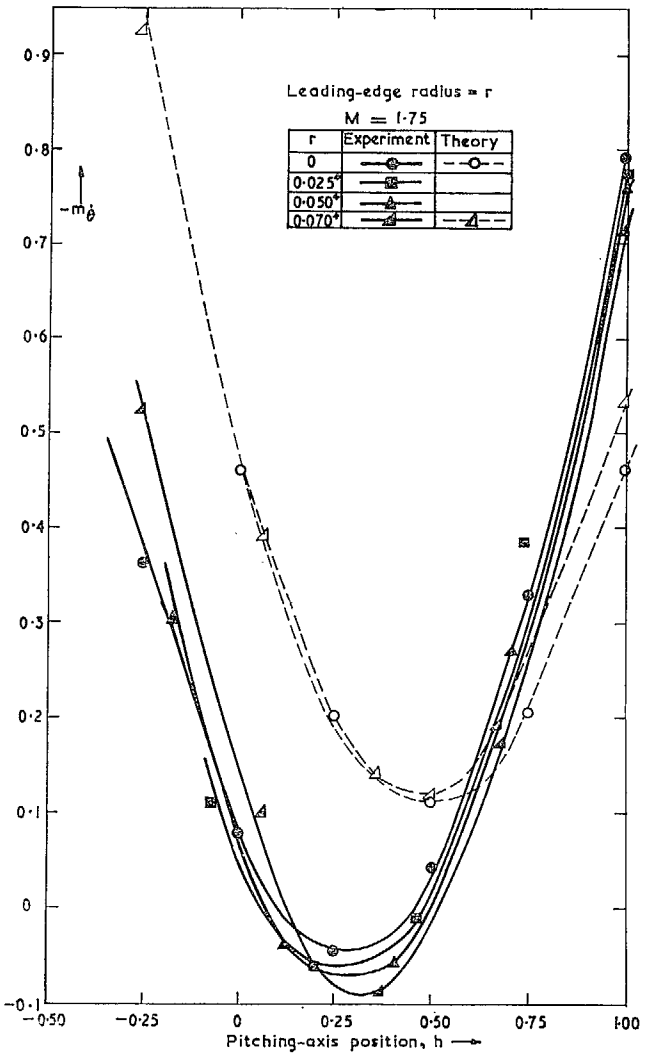

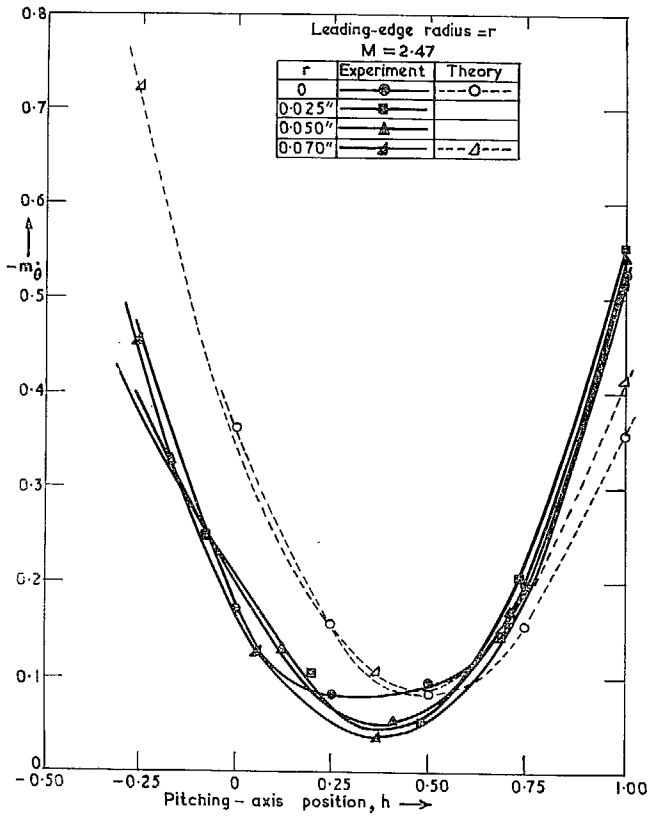

FIGS. 8 and 9. Direct pitching aerodynamic damping ($-m_{\dot\theta}$) for blunt-nosed 24% thick single-wedge aerofoil.

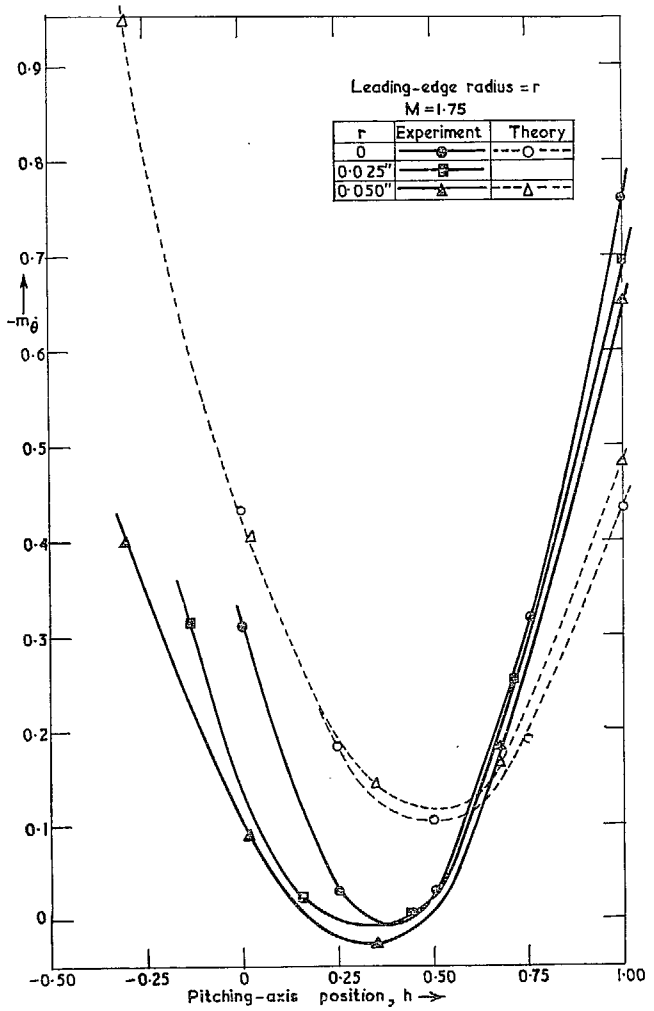

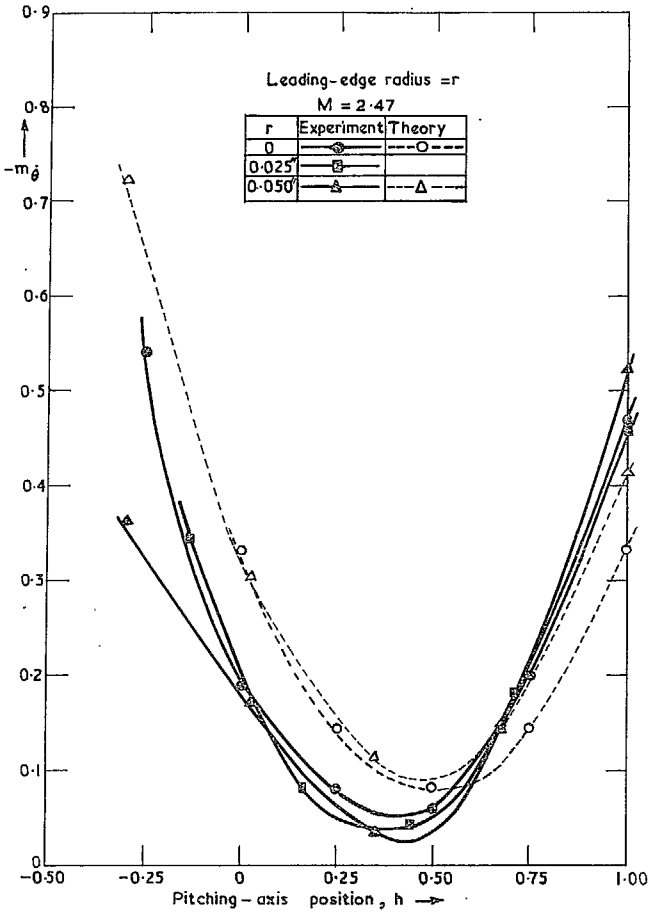

FIGS. 10 and 11. Direct pitching aerodynamic damping ($-m_{\dot{\theta}}$) for blunt-nosed 16% thick single-wedge aerofoil.

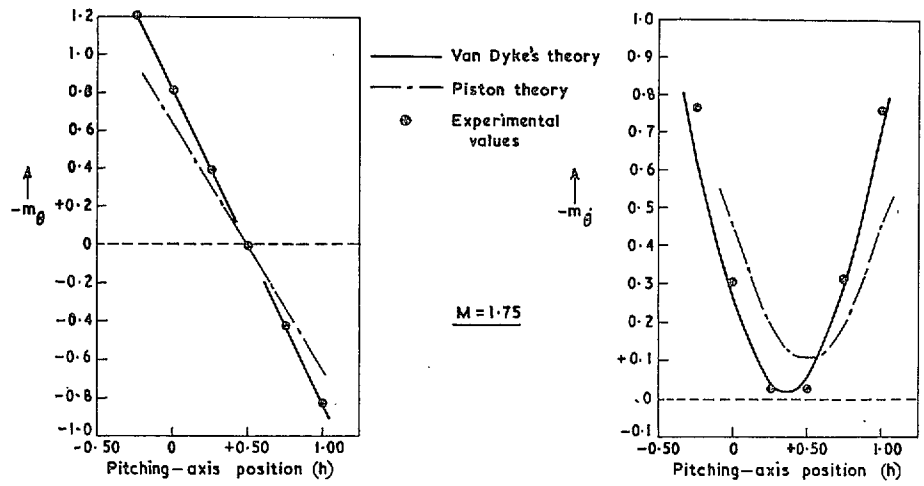

FIG. A1. 16% thick single-wedge aerofoil. ($r = 0{\cdot}0$ in.)

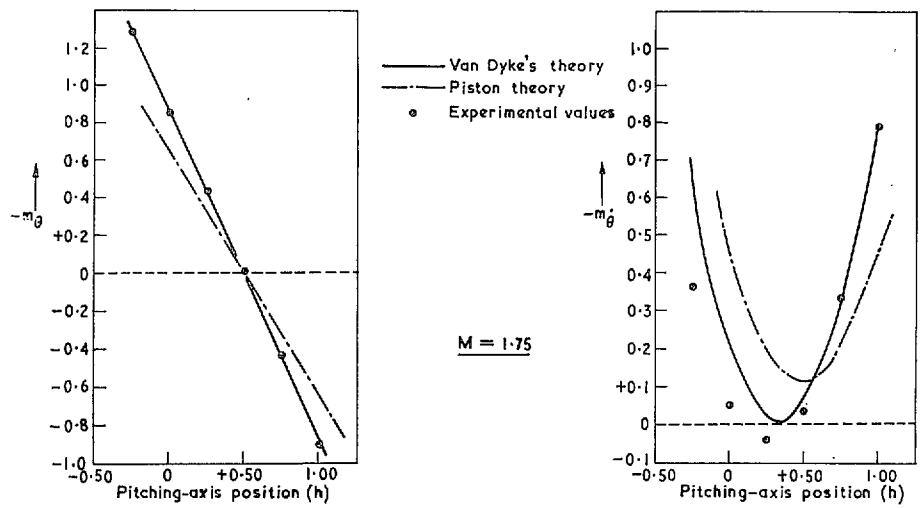

FIG. A2. 24% thick single-wedge aerofoil. ($r = 0{\cdot}0$ in.)

FIGS. A1 and A2. Direct aerodynamic pitching derivatives.

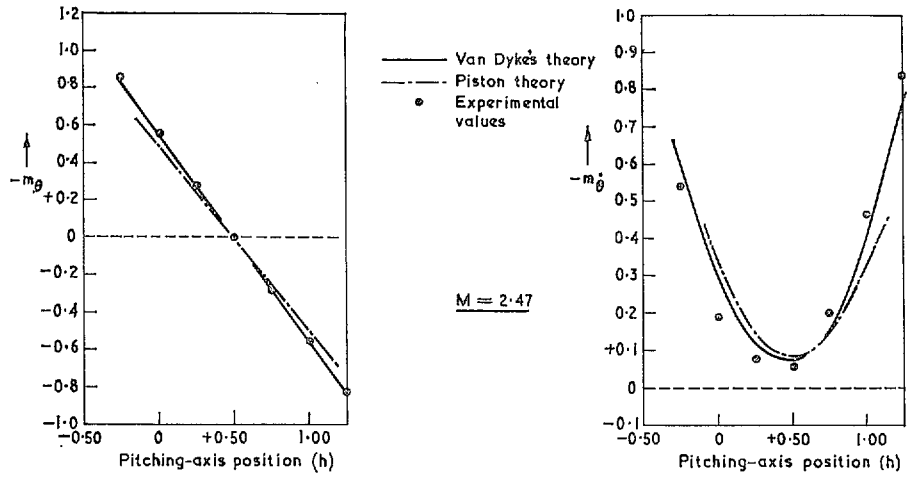

FIG. A3. 16% thick single-wedge aerofoil. ($r = 0{\cdot}0$ in.)

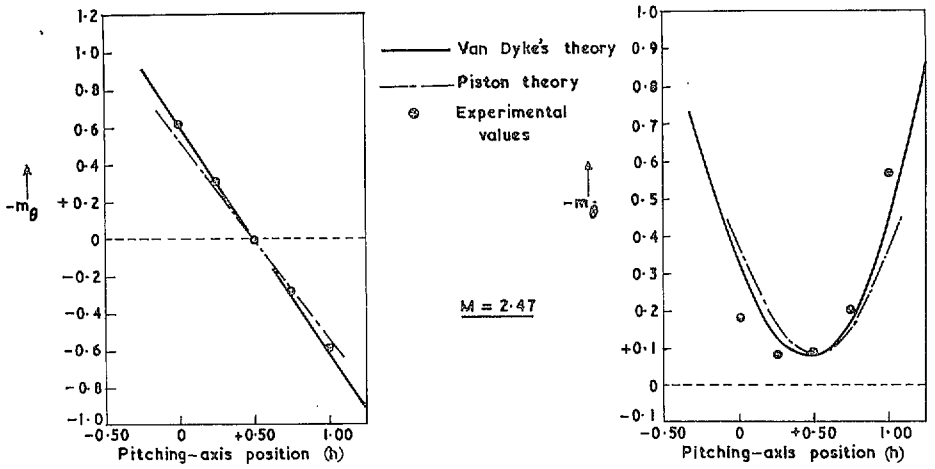

FIG. A4. 24% thick single-wedge aerofoil. ($r = 0{\cdot}0$ in.)

FIGS. A3 and A4. Direct aerodynamic pitching derivatives.

(86603) Wt. 64/1857 K.5 3/63 Hw.

Publications of the Aeronautical Research Council

ANNUAL TECHNICAL REPORTS OF THE AERONAUTICAL RESEARCH COUNCIL (BOUND VOLUMES)

1942 Vol. I. Aero and Hydrodynamics, Aerofoils, Airscrews, Engines. 75*s.* (post 2*s.* 9*d.*)
Vol. II. Noise, Parachutes, Stability and Control, Structures, Vibration, Wind Tunnels. 47*s.* 6*d.* (post 2*s.* 3*d.*)

1943 Vol. I. Aerodynamics, Aerofoils, Airscrews. 80*s.* (post 2*s.* 6*d.*)
Vol. II. Engines, Flutter, Materials, Parachutes, Performance, Stability and Control, Structures. 90*s.* (post 2*s.* 9*d.*)

1944 Vol. I. Aero and Hydrodynamics, Aerofoils, Aircraft, Airscrews, Controls. 84*s.* (post 3*s.*)
Vol. II. Flutter and Vibration, Materials, Miscellaneous, Navigation, Parachutes, Performance, Plates and Panels, Stability, Structures, Test Equipment, Wind Tunnels. 84*s.* (post 3*s.*)

1945 Vol. I. Aero and Hydrodynamics, Aerofoils. 130*s.* (post 3*s.* 6*d.*)
Vol. II. Aircraft, Airscrews, Controls. 130*s.* (post 3*s.* 6*d.*)
Vol. III. Flutter and Vibration, Instruments, Miscellaneous, Parachutes, Plates and Panels, Propulsion. 130*s.* (post 3*s.* 3*d.*)
Vol. IV. Stability, Structures, Wind Tunnels, Wind Tunnel Technique. 130*s.* (post 3*s.* 3*d.*)

1946 Vol. I. Accidents, Aerodynamics, Aerofoils and Hydrofoils. 168*s.* (post 3*s.* 9*d.*)
Vol. II. Airscrews, Cabin Cooling, Chemical Hazards, Controls, Flames, Flutter, Helicopters, Instruments and Instrumentation, Interference, Jets, Miscellaneous, Parachutes. 168*s.* (post 3*s.* 3*d.*)
Vol. III. Performance, Propulsion, Seaplanes, Stability, Structures, Wind Tunnels. 168*s.* (post 3*s.* 6*d.*)

1947 Vol. I. Aerodynamics, Aerofoils, Aircraft. 168*s.* (post 3*s.* 9*d.*)
Vol. II. Airscrews and Rotors, Controls, Flutter, Materials, Miscellaneous, Parachutes, Propulsion, Seaplanes, Stability, Structures, Take-off and Landing. 168*s.* (post 3*s.* 9*d.*)

1948 Vol. I. Aerodynamics, Aerofoils, Aircraft, Airscrews, Controls, Flutter and Vibration, Helicopters, Instruments, Propulsion, Seaplane, Stability, Structures, Wind Tunnels. 130*s.* (post 3*s.* 3*d.*)
Vol. II. Aerodynamics, Aerofoils, Aircraft, Airscrews, Controls, Flutter and Vibration, Helicopters, Instruments, Propulsion, Seaplane, Stability, Structures, Wind Tunnels. 110*s.* (post 3*s.* 3*d.*)

Special Volumes

Vol. I. Aero and Hydrodynamics, Aerofoils, Controls, Flutter, Kites, Parachutes, Performance, Propulsion, Stability. 126*s.* (post 3*s.*)
Vol. II. Aero and Hydrodynamics, Aerofoils, Airscrews, Controls, Flutter, Materials, Miscellaneous, Parachutes, Propulsion, Stability, Structures. 147*s.* (post 3*s.*)
Vol. III. Aero and Hydrodynamics, Aerofoils, Airscrews, Controls, Flutter, Kites, Miscellaneous, Parachutes, Propulsion, Seaplanes, Stability, Structures, Test Equipment. 189*s.* (post 3*s.* 9*d.*)

Reviews of the Aeronautical Research Council

1939–48 3*s.* (post 6*d.*) 1949–54 5*s.* (post 5*d.*)

Index to all Reports and Memoranda published in the Annual Technical Reports

1909–1947 R. & M. 2600 (out of print)

Indexes to the Reports and Memoranda of the Aeronautical Research Council

Between Nos. 2351–2449	R. & M. No. 2450 2*s.* (post 3*d.*)
Between Nos. 2451–2549	R. & M. No. 2550 2*s.* 6*d.* (post 3*d.*)
Between Nos. 2551–2649	R. & M. No. 2650 2*s.* 6*d.* (post 3*d.*)
Between Nos. 2651–2749	R. & M. No. 2750 2*s.* 6*d.* (post 3*d.*)
Between Nos. 2751–2849	R. & M. No. 2850 2*s.* 6*d.* (post 3*d.*)
Between Nos. 2851–2949	R. & M. No. 2950 3*s.* (post 3*d.*)
Between Nos. 2951–3049	R. & M. No. 3050 3*s.* 6*d.* (post 3*d.*)
Between Nos. 3051–3149	R. & M. No. 3150 3*s.* 6*d.* (post 3*d.*)

HER MAJESTY'S STATIONERY OFFICE

from the addresses overleaf

Printed and published by
HER MAJESTY'S STATIONERY OFFICE

To be purchased from
York House, Kingsway, London W.C.2
423 Oxford Street, London W.1
13A Castle Street, Edinburgh 2
109 St. Mary Street, Cardiff
39 King Street, Manchester 2
50 Fairfax Street, Bristol 1
35 Smallbrook, Ringway, Birmingham 5
80 Chichester Street, Belfast 1
or through any bookseller

Printed in England

S.O. Code No. 23-3315